



Modelling compound flooding: a case study from Jakarta, Indonesia

William G. Bennett¹ · Harshinie Karunarathna¹ · Yunqing Xuan¹ · Muhammad S. B. Kusuma² · Mohammad Farid² · Arno A. Kuntoro² · Harkunti P. Rahayu² · Benedictus Kombaitan² · Deni Septiadi² · Tri N. A. Kesuma² · Richard Haigh³ · Dilanthi Amaratunga³

Received: 13 October 2022 / Accepted: 27 April 2023 / Published online: 11 May 2023
© The Author(s) 2023

Abstract

The paper investigates compound flooding from waves, sea surge and river flow in northern Jakarta, Indonesia, which is a global hotspot of flooding, by combining process-based coastal and river models. The coastal hydrodynamic modelling of Jakarta Bay in Indonesia shows that coastal storms can lead to a substantial increase in sea water level due to wind and wave setup in the nearshore areas, including Muara Angke river inlet. The compound flood hazard from a range of flood scenarios was simulated and analysed. The results reveal that low-lying areas around the river inlet are prone to flooding even during regular, low-intensity storm events, while rarer storms caused extensive floods. Floods were not caused by direct overwashing of sea defences but by overspill of the banks of the river inlet due to high sea water level caused by wind set up, wave setup, and sea surge obstructing the drainage of the river and elevating its water level during storms. We also found that the sea level rise combined with rapid land subsidence will inundate the existing coastal flood defences during storms in future. The majority of the city will be below mean sea level by 2100. The overflow of existing coastal defences will lead to extensive flooding in northern, western, and eastern Jakarta unless the defences are upgraded to keep up with future sea level rise.

Keywords Jakarta · Indonesia · Compound flooding · Process-based modelling · Extreme storms · Sea level rise

✉ William G. Bennett
w.g.bennett@swansea.ac.uk

¹ Faculty of Science and Engineering, Bay Campus, Swansea University, Fabian Way, Swansea SA1 8EN, UK

² Bandung Institute of Technology, Jl. Ganesa No. 10, Lb. Siliwangi, Kecamatan Coblong, Kota Bandung, Jawa Barat 40132, Indonesia

³ Global Disaster Resilience Centre, University of Huddersfield, Queensgate, Huddersfield HD1 3DH, UK

1 Introduction

Coastal and inland flooding can be caused by four main source mechanisms: (1) storm surge combined with high astronomical tide (storm tides); (2) locally or remotely (swell) generated waves; (3) fluvial discharge; and (4) direct surface run-off (Hendry et al. 2019). Due to the common meteorological drivers of these mechanisms, they do not often occur in isolation (Bermúdez et al. 2021). Flooding caused by the combination and interaction of one or more of these sources is referred to as compound or coincident flooding (IPCC 2012). The threat posed by compound flooding is particularly prevalent in areas where flooding occurs when high river flows coincide with storm tide and large waves (Lian et al. 2013; Olbert et al. 2017; Petroliaqkis et al. 2016; Tessler et al. 2015; Wahl et al. 2015). At some instances, the severity and consequences of compound flood events can be significantly larger than floods from a single flood driver (Bermúdez et al. 2021; Hendry et al. 2019; Hunt 2005).

The impacts of sea level rise and rapid urbanisation of coastal areas exacerbate the need to understand compound flooding. On a global scale, dependence between storm surge and river discharge and their contribution to compound flooding has been investigated by using observational data (Bevacqua et al. 2017; Eilander et al. 2020; Ward et al. 2018; Lai et al. 2021 and some others) and numerical model simulations (Couasnon et al. 2020), while most studies focused on the regional scale. Wahl et al. (2015) assessed the storm surge and rain fall flood risk in the US. They concluded that the likelihood of compound flood occurrence has significantly increased during the last century at their study sites. For low-lying UK coastal areas, the joint occurrence of skew surges and high river flow has been identified as a frequent phenomenon (Hendry et al. 2019). In addition, it was also found the severity of compound flooding depended on the phase difference and strength of the surge and river flow. In an analysis of the impact compound flooding during tropical cyclones in Haikou City, China, it was found that while storm tide is the primary flood driver, excluding river flow can significantly underestimate flooding (Liu et al. 2022). Future sea level rise (SLR) due to global climate variabilities has found to be a key factor in determining compound flood events in future. Del-Rosal-Salido et al. (2021) examined the effect of SLR on flood defence failures from overtopping and overwashing under compound flooding in Guadalete estuary in the southern Europe. They found that flood defence failure in the estuary can increase by 2000% as a result of SLR. Using a physics-based approach, Gori et al. (2022) showed the joint hazard from simultaneous extreme rainfall and surge in the US will drastically increase from historically to projected future. Thus, compound flooding is an important issue globally that requires investigation under present and future climate conditions.

The frameworks to investigate compound flooding typically include multivariate statistical approaches to characterise statistically significant compound flood drivers (e.g. Camus et al. 2021; Hendry et al. 2019; Ghanbari et al. 2021; Jane et al. 2020; Lucey and Gallien 2022; Kim et al. 2023), coupling of hydraulic and hydrologic or hydrodynamic models to simulate historic or synthetic events (e.g. Gori et al. 2020a; Kupfer et al. 2022; Pasquier et al. 2019), and combining the outputs of statistical modelling with hydraulic models (e.g. Gori et al. 2020b; Shen et al. 2019); . In this paper we investigate compound flooding from river discharge and combined waves, sea surge and tides, in Jakarta, Indonesia. Our approach combines river and coastal hydrodynamic models driven by extreme river flow and coastal storm conditions generated by a simplified statistical approach. The model outputs are then compared to investigate the severity of flooding from simultaneous

occurrence of extreme rainfall and coastal storms of a range of magnitudes and evaluate potential changes to this hazard because of future sea level rise.

Although Jakarta is not subjected to the direct impacts of extreme events such as tropical cyclones and typhoons, regular concurrent coastal and inland flooding in Jakarta causes death and destruction to human lives as well as significant environmental and economic damage (Abidin et al. 2010; Sagala et al. 2013; Ward et al. 2013). The National Disaster Management Authority of Jakarta (BNPB) reports 74 flood incidents during 2020 and 2021 alone which affected 98,800 residents and led to 24 fatalities, with damage cost calculated around US\$ 71 million. However, this loss is smaller than that from the previous mega flood event in 2007 which was estimated at US\$ 970 million, and from the event in 2002 which was estimated at US\$ 960 million (Priyambodoho et al. 2021). In 2013, a major flood event inundated 124 villages and 98,000 houses, displaced 40,000 people, killed 20 people, with a total estimated economic damage worth US\$ 775 million (Wijayanti et al. 2017). Hanson et al. (2011) project that Jakarta will be ranked 20th of 136 port cities in terms of population exposed to flooding by 2070. In a similar study, Hallegatte et al. (2013) find Jakarta will be in the 11th place for annual expected loss, taking into account the impacts of socio-economic change, subsidence, sea level rise, and adaptation by 2050. By simulating the potential impacts of future sea level rise and land subsidence, Ward et al. (2011a, b) found that the economic impacts of flooding in Jakarta may increase by a factor of 4–5 between 2010 and 2050. This is predominantly due to the impacts of land subsidence on flooding. The need to evaluate current and future compound flooding in Jakarta is well established.

2 Study site: Jakarta, Indonesia

Jakarta is the economic, political, and cultural capital and the largest city in Indonesia. It has been identified as a global hotspot for flooding hazards (Wicaksono and Herdiansyah 2019). The city is located on the northwest coast of Java, in Jakarta Bay, and covers an area of 662 square kilometres (Akmalah and Grigg 2011) (Fig. 1a). Jakarta Bay is an open bay (Fig. 1a) with maximum water depths not exceeding 60 m (Surya et al. 2019). The tides in the bay are diurnal (Defant 1961) with a maximum range of approximately 1 m, with 0.6 m highest level and a low of -0.4 m relative to mean sea level during spring tides (Surya et al. 2019). The tidal currents inside the bay are mainly below 0.2 m/s, with peak currents occurring at and near river mouths (Rusdiansyah et al. 2018). Ebb currents near river mouths are slightly larger than the flood currents due to the river discharges. Based on the results of a numerical modelling study using 10 years' worth of hourly wind data, Larasari et al. (2018) estimated offshore design significant wave height (H_s) of 4.31 m and peak period (T_p) of 8.85 s. Waves measured in Jakarta Bay at [106.76E, 6.01S] during January–February 2017 give H_s values between 0.3 and 1.1 m (Adytia et al. 2022).

Jakarta covers an area of 662 square kilometres (Akmalah and Grigg 2011) (Fig. 1a). It has suffered from rapid population growth and urbanisation beyond the capacities of national and local governments. The population in Jakarta had reached 11.4 million by 2018, with the Greater Jakarta area alone reaching 34 million (Rustiadi et al. 2021). Urbanisation has led to inadequate housing, infrastructure, and healthcare, poverty, and high rates of unemployment (Akmalah and Grigg 2011). Thirteen rivers pass through the city area (Abidin et al. 2001; Mishra et al. 2018). It undergoes rapid and persistent land subsidence as a result of large-scale extraction of groundwater, increased loading from rapidly increasing building construction, as

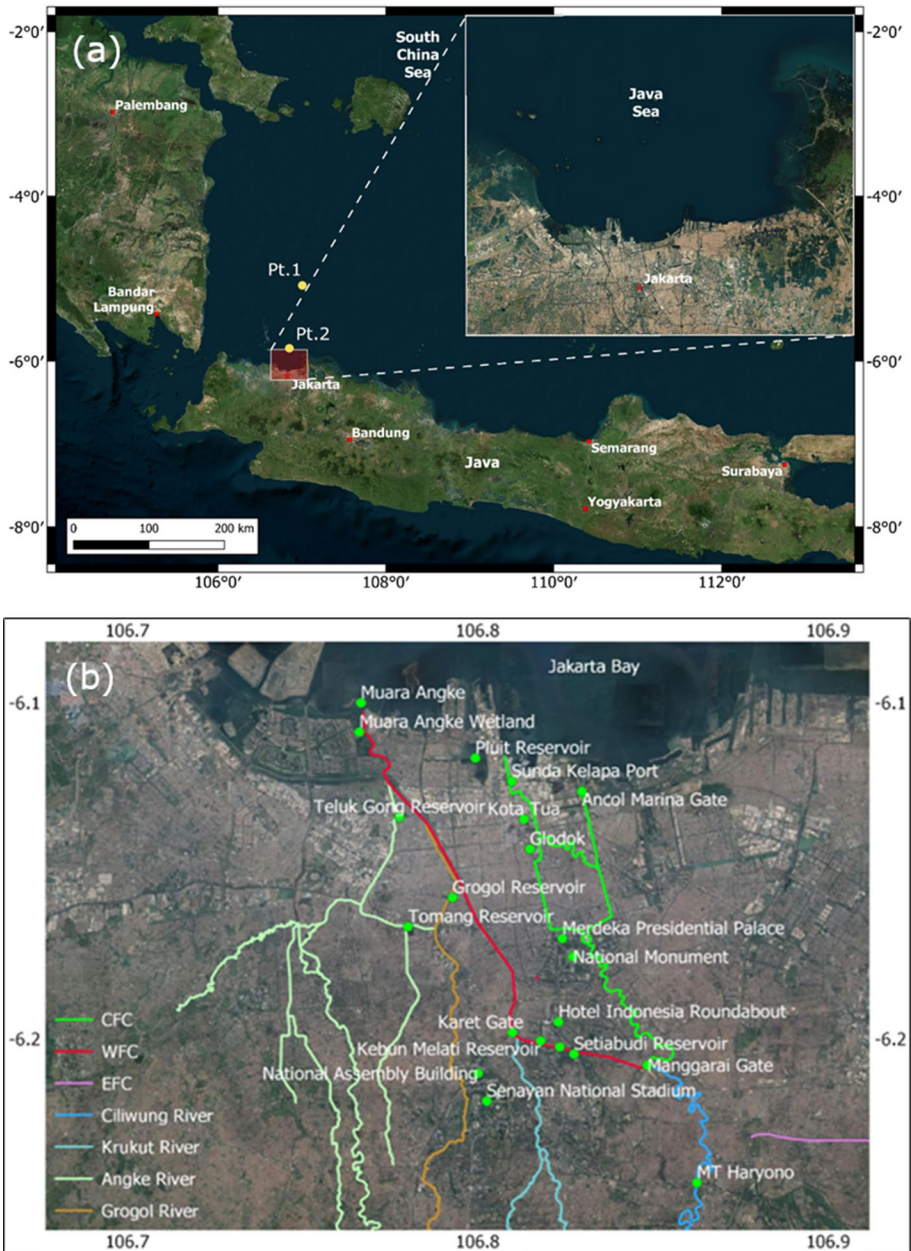


Fig. 1 a Location of Jakarta Bay, Indonesia and the city of Jakarta. Pt.1 and Pt.2 indicate the locations of ERA5 wave (Hersbach et al. 2018) and National Oceanic and Atmospheric Administration wind data used, respectively; b a map of the river and drainage canal system in the west Jakarta including Ciliwung river, West Flood Canal (WFC), Muara Angke river inlet

well as natural consolidation and geotectonic adjustments. The combination of land subsidence and sea level rise due to global climate change have significantly exacerbated flooding in Jakarta (Abidin et al. 2010).

Flooding in the inland areas of Jakarta is caused by high rainfall events generated by tropical depressions and persistent low level wind convergence created by cross-equatorial northerly surge (Lubis et al. 2022). Obstructed waterways, deforestation, and a lack of adequate drainage and flood control provision exacerbate inland flooding (Akmalah and Grigg 2011; Budiyo et al. 2016; Emam et al. 2016; Farid et al. 2021; Kusuma et al. 2010). Although alternative solutions for river floods, such as diversion canals, increasing capacity, and other measures have been investigated, problems with land acquisition and construction costs remain the most significant obstacles to find an effective flood mitigation solution (Formánek et al. 2014).

Low-lying coastal areas in the north-west of Jakarta are also being regularly flooded. The same weather conditions that drive heavy rainfall inland causes locally generated high waves and sea surge in Jakarta Bay, which when combined with high river runoff, lead to compound flooding in low-lying northern Jakarta. Although some areas of the northern Jakarta Bay coastline have been protected by a range of adaptation measures to counter coastal inundation, such as construction of sea walls, flood water pumping stations and tidal gates (Deltare 2009) many low-lying areas surrounding Muara Angke river inlet (Fig. 1b) are still exposed. The threat of tidal inundation has led to existing sea walls being strengthened and replaced recently. However, due to the substantial rates of subsidence some supposedly protected areas are also becoming increasingly flood prone (Rusdiansyah et al. 2018).

Approximately 3.5 million slum dwellers in low-lying coastal areas surrounding Muara Angke river inlet in north-Jakarta, are subjected to frequent flooding (Texier 2008; Van Voorst and Hellman 2015). This river inlet is fed by the flood water from Ciliwung River, which is diverted to the West Flood Canal (WFC) at Manggarai gate. Manggarai flood gate regulates water flow entering the WFC, and the Manggarai-Cikini flood gate controls water flow to Central Jakarta through the Central Flood Canal (CFC). The water flow through the Manggarai-Cikini sluice gate is restricted so as not to flood the Central Jakarta Area through the CFC and diverts most of the Ciliwung River discharge into the WFC. CFC is the original channel of the Ciliwung River which flows through Central Jakarta and branches to two gated estuaries (Pluit, Ancol) which are part of the Pluit polder system (Fig. 1b). In addition to flow diverted from the Ciliwung river, the WFC collects water from several other rivers (Krukut River, Grogol River, and Angke River) before eventually emptying into Jakarta Bay through Muara Angke river inlet (Fig. 1b). Both Ciliwung River and WFC overflows regularly during high rainfall events.

Muara Angke, which floods from both overspill from the WFC and from the sea, is the focus of our study. Although previous studies report inland (e.g. Budiyo et al. 2015) and coastal (e.g. Ward et al. 2011a) flooding in isolation no studies on compound flooding from the simultaneous occurrence of inland and coastal storms were reported, despite them frequently inundating Muara Angke.

3 Modelling methodology

The methodology combines numerical simulations of coastal and river flooding to investigate compound flooding in Jakarta. Here, the storm wave heights and water levels required to determine the coastal boundary condition for compound flooding were derived from a

numerical coastal wave and hydrodynamic model of Jakarta Bay. The model was set up using the open-source Delft3D coastal modelling software (Lesser et al. 2004). The inland flow and flooding surrounding the WFC was modelled using the HEC-RAS river analysis system (<https://www.hec.usace.army.mil/software/hec-ras/>) of the Ciliwung River including the West Flood Canal and Muara Angke river inlet (Fig. 1b). The downstream water level boundary condition to the river model was provided by Jakarta Bay coastal model while the upstream boundary conditions were provided by river discharge hydrographs. Historic evidence suggests that simultaneous occurrence of inland and coastal storms is a regular event in Jakarta (Jamalludin et al. 2016). Therefore, all simulations in this study considered coastal and inland storms are driven by the same meteorological event and hence coastal storm and river flood peaks occur simultaneously. The detailed modelling procedure is given below.

3.1 Coastal storm boundary conditions

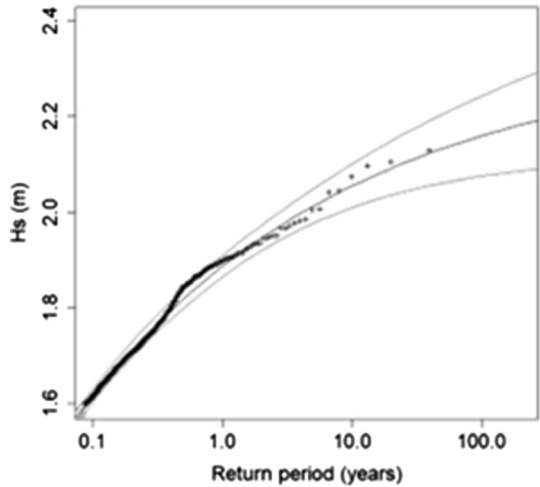
The Jakarta Bay coastal model was driven by storm wave and water level inputs at the offshore boundary of the numerical model domain. Time-varying but spatially constant wind velocity and direction were provided within the model domain. It was decided to investigate the impacts from frequent as well as rare, extreme storms, as over time frequent storms can cause nuisance flooding which can lead to similar impacts as individual extreme flood events (Moftakhari et al. 2018). On this basis, it was decided to simulate storms with a range of return period conditions between 1 in 1 year and 1 in 100 years.

Although Gori and Lin (2022) demonstrated the advantages of using a probabilistic approach to evaluate compound flood hazard, it was not feasible to conduct a multivariate statistical analysis to determine statistically significant compound flood drivers due to the lack concurrent datasets on variables defining compound floods in Jakarta (wave height/wave period, storm surge, river flow). As such, univariate statistical analysis was performed on each individual variable, using the limited available data, to generate the variable with a range of return periods. They were then combined systematically to develop plausible flood scenarios, which will serve as input boundary conditions to the coastal and river hydrodynamic models to simulate combined floods. We recognise that this approach does not capture the dependency between the individual variables in time and space although it overcomes the limitations of the data availability while allowing us to investigate ‘worst case scenario’ combined floods from a spectrum of input conditions. Due the nature of the extreme socio-economic issues relating to flooding in Jakarta, this cautious approach will still provide useful insights for risk-averse development of coastal and flood risk management options. *Storm waves*: Due to a lack of local measured data, wave projections from the nearest European Centre for Medium-range Weather Forecast (ECMWF) ERA5 dataset (Hersbach et al. 2018) were used to determine various return period wave conditions at the offshore boundary of the numerical model domain (Fig. 3) to drive the numerical model. ERA5 dataset provided hourly wave conditions (significant wave height, mean period, and predominant direction) at $0.5^\circ \times 0.5^\circ$ resolution between 1979 and 2018. Waves at the nearest output point (-5° N, 107° E) to the offshore boundary of the model domain were used. To determine extreme conditions with a range of severity levels for developing storm scenarios for numerical model simulations, the Generalised Pareto Distribution (GPD) (Eq. 1) was selected. The GPD has been used in several studies to investigate extreme wave heights (Alsaq and Shamji 2022; Guo et al. 2020; Niroomandi et al. 2018; Pender and Karunarathna 2013) and wind speeds (Guo et al. 2020; Jagger and Elsner 2006; Machado

Table 1 Extreme storm wave conditions used to drive the numerical wave model of Jakarta Bay

Storm parameters	Storm event return period			
	1 in 1	1 in 10	1 in 50	1 in 100
H_s (m)	1.89	2.05	2.13	2.16
Wd_{avg} (°)	320	320	320	320
T_m (s)	4.74	4.74	4.74	4.74

Fig. 2 GPD profile for significant wave height. Crosses indicate storm significant wave height values, with the GPD fit and 95% confidence intervals indicated by the three curves



and Calliari 2016) and was fit to the significant wave height data of ERA5 following the method of Hawkes et al. (2002).

$$Pr\{X > x|X > u\} = \begin{cases} 1 + \xi\sigma^{-1}(x - u)^{-\frac{1}{\xi}} & \xi \neq 0 \\ e^{-\frac{x-u}{\sigma}} & \xi = 0 \end{cases} \tag{1}$$

In Eq. (1), x is the significant wave height H_s , σ and ξ are scale and shape parameters, respectively, and u is the threshold that ensures model convergence (Coles 2001). The average wave period (T_m) from the model outputs was used, with a predominant wave direction (Wd_{avg}) from the Northwest. The resulting significant wave height, mean period and predominant wave direction are given in Table 1, with the GPD profile displayed in Fig. 2.

Wind: Wind data during storms were determined from the National Oceanic and Atmospheric Administration (NOAA) data provided at six-hourly intervals at (− 5.9201° N, 106.875° E) (Fig. 1). Eighteen years worth data from 01/01/2000 to 31/12/2018 was used. As with the wave conditions, the GPD was fitted to the wind data to provide extreme wind speeds and directions, which are summarised in Table 2. To generate time varying storm wind and wave conditions, a three-point spline shape is used (Fig. 3a), where the start and end of the storm are the threshold for model convergence, and the peak wave or wind occurs at the mid-point.

Water levels: The tidal variations at the open boundaries of the model domain were derived using tidal constituents obtained from TPXO 8.0 OSU Tidal Inversion Software (Egbert and Erofeeva 2002). From this, the highest astronomical tidal curve was extracted

Table 2 Extreme wind speeds used to drive the numerical wave model of Jakarta Bay

Wind parameters	Storm event return period			
	1 in 1	1 in 10	1 in 50	1 in 100
Velocity (m/s)	20.21	29.23	35.77	38.65
Predominant direction (°)	315	315	315	315

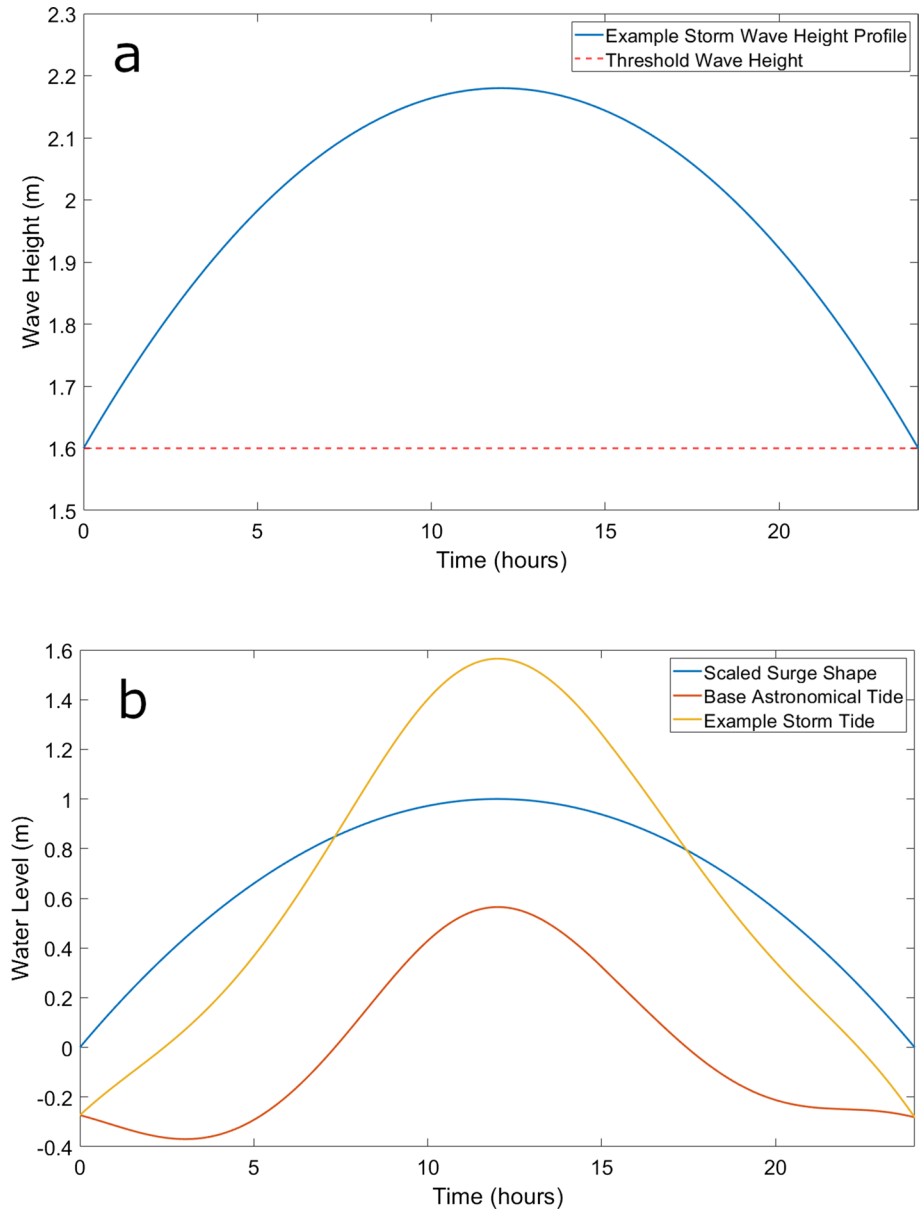


Fig. 3 An example of **a** offshore storm profile; **b** time-varying surge profile on the base astronomical tide

to provide the base for storm water levels. As no long-term tide gauge records were available at Jakarta Bay to calculate storm surge levels, 0.5 m, 0.75 m and 1 m peak storm surge values due to atmospheric pressure representing low, medium and high storm surge conditions were selected. These values were selected on the basis that 0.5 m surges are a regular occurrence and that surges higher than 1.0 have not been reported in Jakarta Bay. As with the method of McMillan et al (2011), to create a storm water level profile, a time-varying surge profile encompassing the period of the storm was constructed and added to a base tidal water level variation curve between mean high-water spring (MHWS) and highest astronomical tide (HAT). The shape of the time variation of storm and surge during the course of a storm was determined using a three-point spline curve, with the surge peak equal to the desired surge level. The addition of the surge profile to the base tidal curve provided the total storm water level time series at the offshore boundary during the modelled storm events. In combining the two, it was assumed that the surge peak coincides with the highest tidal water level, producing the worst-case water level scenario. The storm duration used for all combinations was 24 h. An illustration of storm, surge and tide profiles used in numerical simulations are shown in Fig. 3b.

To investigate future hydrodynamic conditions at Jakarta Bay due to global climate change, sea level rise (SLR) in particular, the water levels in the model were modulated by the rise in regional sea level and land subsidence. The RCP 4.5 and 8.5 scenarios (Moss et al. 2008, 2010) were selected providing the moderate and most extreme SLR projections. Using the dataset provided by Oppenheimer and Glavovic (2019), this gives median estimated projected SLR values of 0.551 m (lower bound=0.328 m, upper bound=0.803 m) and 0.875 m (lower bound=0.591 m, upper bound=1.23 m) for 2100 for the RCP 4.5 and 8.5 scenarios, respectively. Though these values are estimated projections, the uncertainty means they may be larger and may cause further issues that are not considered here (Gori and Lin 2022). Those values were added to the surge subset of the model runs. It was assumed that peak wave heights and mean wave periods of the current storms remain unchanged in future, considering the fact that no significant changes to future wave conditions were found in the equatorial regions of the Indian Ocean (Bhaskaran et al. 2014).

3.2 Coastal hydrodynamic modelling

The Delft3D coastal modelling suite has been extensively used in both industry and academia to simulate hydrodynamics (FLOW module) and waves (WAVE module) in a wide range of coastal environments. This is in part due to its capability to simulate waves, hydrodynamics, sediment transport, morphological evolution, ecology, and water quality. Considering this functionality, several studies have utilised Delft3D to investigate compound flooding (e.g. Del-Rosal-Salido et al. 2021; Kumbier et al. 2018; Kupfer et al. 2022; Muñoz et al. 2022). In this study, Delft3D FLOW and WAVE modules were online coupled to correctly capture wave-tide interactions. The 2D depth averaged FLOW module is utilised, solving the unsteady shallow water equations with the hydrostatic pressure assumption.

To transform waves from the ERA5 output location to Jakarta Bay, it was necessary to create two model domains: a large domain covering Jakarta Bay and the surroundings, which extended offshore; and a small domain of Jakarta Bay (Fig. 4). Both domains use curvilinear grids constructed using the RGFRID software, to refine the grid cells into areas of interest (Deltares 2022). In the larger domain (Fig. 4a), the grid cells at the offshore boundary are approximately 2400 m × 2200 m. The grid cells were gradually refined to 1100 m × 1100 m at the seaward boundary of the nested small domain (Fig. 4b). The

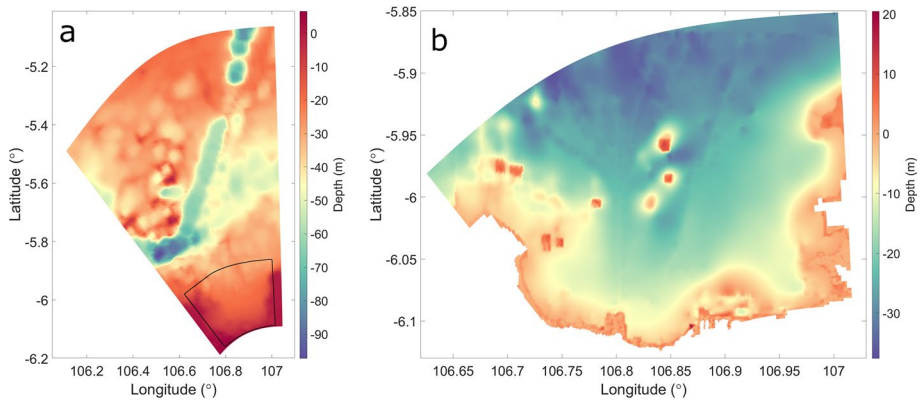


Fig. 4 Delft3D numerical model domains and model bathymetry of Jakarta Bay. **a** Large scale domain; **b** high-resolution small, nested domain of Jakarta Bay

offshore boundary of the larger domain is positioned at a ERA5 data output point, and at a sufficient depth to ensure smooth transformation of the waves at the boundary. The grid cell size of the nested small domain gradually refines from 200 m × 350 m at the seaward boundary to 120 m × 70 m along the coastline of the Bay to provide higher resolution outputs in the nearshore areas. Bathymetric data for the two model domains were taken from GEBCO 2019 global dataset (GEBCO Compilation Group 2019) at 15 arc second resolution, and more local Jakarta Bay data at 180 m resolution. Both datasets have mean sea level as the vertical datum.

The numerical coastal model was calibrated using a range of values of uniform Chezy roughness coefficient and validated against water level data from the Ancol tide gauge located in Jakarta Bay during the period from 01/09/2019 to 18/09/2019. The tide gauge is located at (− 6.126N, 106.830E) at a water depth of 1.69 m. The comparison of simulated and measured water levels is shown in Fig. 5. A Chézy roughness coefficient of 0.65 m^{1/2}/s was used. The results reveal that the simulated water level variation is in very good agreement with measured data with R^2 value of 0.8, and a root mean square error (RMSE) of 0.09 m. It should be noted that measured wave data was not available in Jakarta Bay to validate wave simulations. However, the average wave height at the flood-prone shoreline of Jakarta Bay is small due to the predominant north-westerly wave approach. Coastal flooding around Jakarta Bay is predominantly generated by storm tide.

The validated coastal model was used to simulate time- and space-varying storm wave heights and water levels in Jakarta Bay from storms with return periods given in Table 1 combined with three surge levels 0.5 m, 0.75 m and 1.0 m for both current and future sea levels.

3.3 Compound flood modelling

Compound flood simulation in Jakarta was carried out using the 1D-2D coupled model developed in HEC-RAS (<https://www.hec.usace.army.mil/software/hec-ras/>) flood modelling software. The model utilised a Digital Elevation Map (DEM) of the Jakarta area (Badan Informasi Geospasial 2018), which was further refined using field measurements

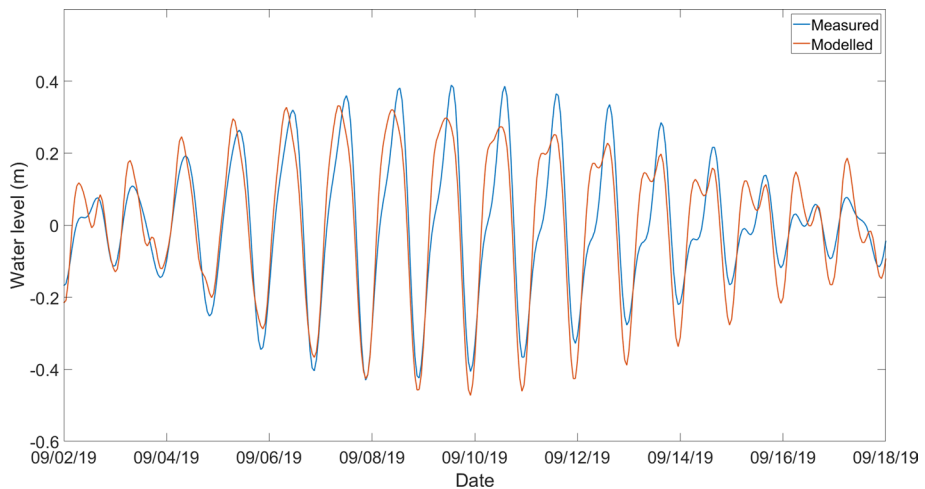


Fig. 5 Validation of Jakarta Bay hydrodynamic model against measured water level data by Ancol tide gauge located at Jakarta Bay during the period from 01/09/2019 to 18/09/2019

of Ciliwung River and WFC as the basis for the geometry of the model (Formánek 2014). The DEM used is the national DEM map (DEMNAS) with a resolution of 8.5 m based on DSM not DTM, so the elevation captured is surface elevation, including elevation of trees, buildings and seawalls (<https://tanahair.indonesia.go.id/demnas/#/>). The model domain comprises of the area between the Ciliwung River from Haryano at the upstream and Muara Angke river inlet mouth at the downstream (Fig. 1b). The flow and water level at the upstream model boundary to run numerical simulations were provided by a stream-flow hydrographs of Ciliwung River and Krukut River. Limited availability of temporal hydrograph data for the Ciliwung River resulted in determining the discharge hydrograph using the rainfall-runoff model using the synthetic hydrograph method based on Indonesian National Standard (SNI 2415-2016). The stream-flow hydrographs used in this study are the discharge hydrographs of 1 in 2 year (Q2), and 1 in 100 year (Q100) return period. Those were systematically combined with the sea water levels determined from the coastal storm model in Sect. 3.2 at the mouth of the Muara Angke river inlet (the downstream model boundary) for 1 in 1 year (W1), and 1 in 100 year (W100) return period coastal storms to develop compound flood scenarios. It should be noted that Q2, W1 and Q100, W100 resembles ‘regular’ and ‘extreme’ conditions. It should be noted that 1 in 100 events in this case, are considered as the ‘worst-case’ scenario for this study. To simulate future compound flooding in Jakarta, a selection of inland and coastal storm scenarios was combined with 1 m surge added to 2100 relative sea level from RCP 8.5 climate change scenario. The relative sea level in 2100 was determined by modifying the absolute 2100 sea level calculated using the RCP8.5 climate scenario by the average land subsidence rate in Jakarta. It should be noted that only the worst possible future flood scenarios were modelled (Table 3).

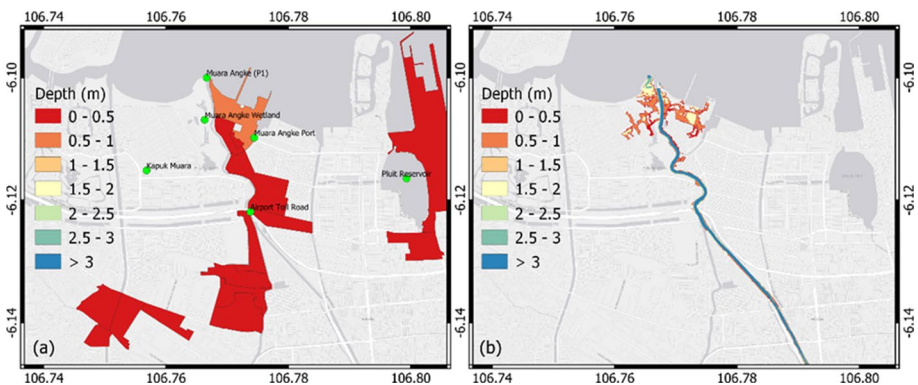
3.4 Compound flood model validation

Before applying the HEC-RAS Jakarta flood model for generating flood maps from the selected combined river flow, water level, and storm conditions, the model was validated

Table 3 A summary of statistical coastal and inland flood variables used to develop compound flood scenarios

Flood variable	Current climate	Future climate
Storm wave height and wind speed	W1 (1.89 m, 20.21 m/s)	W1 (1.89 m, 20.21 m/s)
	W100 (2.16 m, 38.65 m/s)	W100 (2.16 m, 38.65 m/s)
River flow	Q2 (223 m ³ /s)	Q2 (223 m ³ /s)
	Q100 (563 m ³ /s)	Q100 (563 m ³ /s)
Storm surge	0.5 m	0.5 m
	0.75 m	0.75 m
	1.0 m	1.0 m
Land subsidence	–	10 cm/year
SLR	–	RCP4.5 (0.7 cm/year)
	–	RCP8.5 (1.0 cm/year)

by qualitatively comparing simulated and observed flooding from a storm event that took place in Jakarta in November 2020. The input discharge hydrographs of Ciliwung River at Manggarai Gate, Krukut River at Karet Tengsin gauge and the sea water level at Pasar Ikan Station of Sunda Kelapa Port were provided by the Provincial Water Resources Agency of Jakarta, Dinas Sumber Daya Air (DSDA) to simulate the November 2020 flood. The discharge hydrographs were used as the upstream boundary condition, and the measured sea water level as the downstream boundary condition. The simulated flood map was qualitatively compared with the observed flood map of this event (Fig. 6). Quantitative observations of flood inundation during this event or any other past event were not available. Also, it should be noted that the observed flood maps have been developed using a limited number of spot measurements and applying the ‘bathtub’ approach to create the flooded areas, providing only a crude approximation of the flood-affected areas. As a result, quantitative validation of the flood model was not possible. However, the simulation result was qualitatively comparable to the observed data at the low-lying coastal areas around the east bank of the Muara Angke river inlet. Flood measurements were not available in the west bank area of the river inlet. Observational data obtained from the Jakarta Water Resources

**Fig. 6** A comparison of observed and simulated flood maps from the 16 November 2020 storm (a) observed data from DSDA Jakarta (b) HEC-RAS model simulation

Service showed that flooding occurred within the Rukun Warga administration, not as a delineation for the floods that occurred, so that the flood inundation appears larger than it should be. It should be noted that the model simulated only the compound flooding in low-lying Muara Angke area. Therefore, observed floods in other areas of Angke River, part of Teluk Gong Polder, Ancol and Cengkareng are not compared.

4 Results and discussion

The storm-induced hydrodynamics in Jakarta Bay from a wide variety of frequent and rare coastal storms is presented and discussed, and compound flooding from the simultaneous occurrence of inland and coastal storms is discussed focusing mainly on the low-lying coastal areas surrounding the Muara Angke river inlet and the West Flood Canal.

4.1 Storm-induced hydrodynamics in the nearshore areas of Jakarta Bay

Peak storm wave heights in Jakarta Bay from a subset of the modelled storm scenarios, together with 1 m sea surge, are shown in Fig. 7. For all storm events, the highest wave heights occur offshore as expected. In the nearshore, the western side of the bay is more sheltered than the east. For the W1 wind and wave conditions (Fig. 7a), the peak storm wave heights are approximately 4 m offshore, which decreases to 2.5 m near the -5 m depth contour in the southeast and between 1.5 and 2 m on the south-western side of the bay. For W10 storm (Fig. 7b), the largest waves in the offshore exceeded 6 m. 3.0 m high waves are found along the -5 m depth contour in the eastern side of the bay while 1.5–2.0 m waves are found in the south-west. The maximum wave height found in the south-western side of the bay is 1.8 m (Fig. 7b). The W100 storm resulted in significantly larger waves along the -5 m depth contour varying from 3–4 m at the south-eastern side of the bay to 2–3 m at the south-western side (Fig. 7c). Wave heights in all cases rapidly diminished when they become depth limited in the surf zone.

The peak water levels corresponding to the cases shown in Fig. 7a–c are shown in Fig. 7d–f, respectively. The total water level includes highest tide, storm surge and wind set up. Wind setup is generated by the strong wind shear stress acting on the sea surface. Since wind is directed shoreward in this case, for a given storm, wind setup increases towards the nearshore areas. The wind set up increases with the increase in storm severity due to increase in wind speed. Although the maximum storm surge was kept at a constant value of 1 m above the highest tide in all simulations, wind set up combined with wave setup (in the surf zone) contributed to increase the water level with the increase of the severity of the storm. With the regular W1 storm event (Fig. 7d), the peak storm water level along the -5 m depth contour is fairly constant at 1.6 m above mean sea level, with only a slight increase to 1.8 m towards the southeast side of Jakarta Bay. During more extreme W10 and W100 events (Fig. 7e, f), a marked increase in nearshore water level can be seen. During the W10 storm, peak water level increases from 2.0 m offshore, to 2.2 m in the southwest, and 2.5 m in the southeast along the -5 m contour (Fig. 7e). This further increases to 3.5 m in the east side of the bay. During the W100 storm, nearshore peak water level along the -5 m contour changed from 2.5 to 3.0 m from south-west to south-east of the bay (Fig. 7f).

Climate change can significantly increase global sea levels. It has been projected that in sea level rise of approximately 1 cm/year and 0.6 cm/year will take place around Indonesia

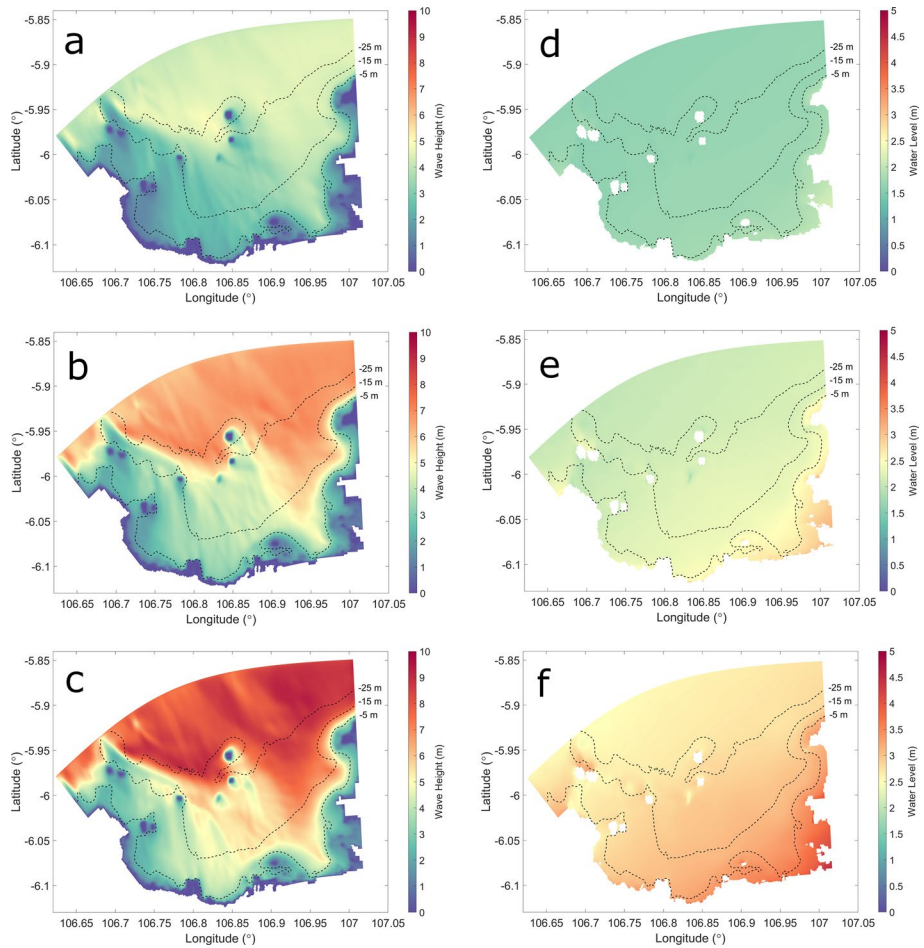


Fig. 7 Peak storm wave heights (a–c) and water levels (d–f) at Jakarta Bay during four storms W1, W10, and W100, respectively, with 1 m surge

under RCP8.5 and RCP4.5 climate change scenarios, respectively. This will result in an absolute sea level rise of 0.875 m (RCP8.5) and 0.551 m (RCP4.5) in Jakarta Bay by 2100 (Oppenheimer, Glavovic 2019). The simulated peak wave heights and water levels in 2100 in Jakarta Bay under the RCP 8.5 climate change scenario are shown in Fig. 8. For clarity, in these simulations, storm wave conditions at the offshore and surge were kept the under the ‘present’ conditions, assuming that atmospheric and offshore wave conditions will not change significantly in future, while the sea level was adjusted to include sea level rise from RCP 8.5 scenario. Although the pattern of spatial variation of peak wave height from all four storms remains largely similar to that of without sea level change (Fig. 7), an overall 0.4–0.6 m increase can be seen along the – 5 m contour across the bay in all simulation scenarios as shown in Fig. 8a–c.

Peak storm water levels corresponding to the cases in Fig. 8a–c are shown in Fig. 8d–f. The increase in sea level of 0.875 m for the RCP 8.5 scenario provides broadly the same increase in the peak storm water level for all simulated scenarios. This is expected as

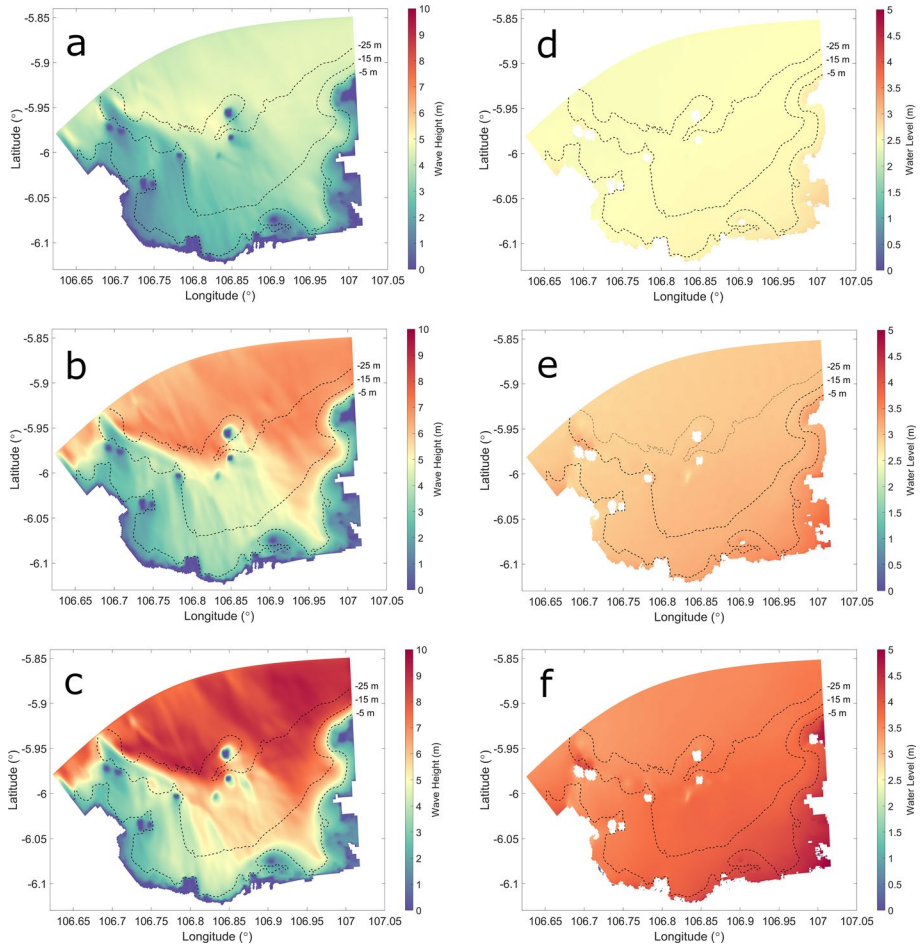


Fig. 8 Peak storm wave heights (a–c) and water levels (d–f) at Jakarta during four statistically significant storms W1, W10, and W100, respectively, in 2100, with 1 m surge and RCP8.5 sea level rise

climate change impacts on the storm surge and the incident storm wave conditions were not considered in the simulations.

Three locations at sea front which are extremely vulnerable to rise in water level and wave height in Jakarta Bay were selected to investigate further: P1, located at the mouth of WFC with a seabed depth of -0.52 m; P2, in front of the flood defence seawall situated to the east of the river mouth with a bed depth of -5.3 m; and P3, further east at a location where the land protrudes from the coastline with a bed depth of -8.6 m (Fig. 9).

Peak wave height and water levels during twenty coastal storm scenarios at those three locations are shown in Fig. 10. Although some small differences can be seen, the peak water level from a given storm scenario at all three locations are widely similar. The highest peak water level (4.1 m) was from the W100 storm when combined with 1.0 m surge and sea level from RCP8.5 climate change scenario. It has been found that the current crest height of the seawall at P2 and P3 are 4.8 m above the present mean sea level, which is only marginally above the peak water level from the future W100 storm scenario with RCP8.5



Fig. 9 Individual output point locations selected to closely examine wave heights and water levels along the south-east shoreline of Jakarta Bay

SLR scenario and 1 m surge. It should be noted that land subsidence, which is a widely reported phenomenon in Jakarta, was not taken into account in these simulations.

Although the peak water levels from the simulated storm scenarios are similar at all three locations, peak storm wave height shows notable spatial variability which can be attributed to the seabed bathymetry around those points and the approach wave direction. When the storm severity varies from the lowest (W1 storm with 0.5 m surge) to the highest (W100 storm with 1 m surge and SLR due to RCP8.5), a 30–50% increase in peak storm wave height can be seen at P1, 3–10% at P2 and 6–8% at P3, thus showing a greater impact of SLR on the wave height.

4.2 Compound floods in Jakarta

Figure 11 shows flooding from Q2 inland storm combined with a range of coastal storms. Figure 11b is the baseline scenario where river and estuarine floods are not impacted by a coastal storm. Figure 11c–e shows flood inundation from Q2 combined with W1, and W100, but without sea surge.

The comparison of the three compound flood cases in Fig. 11c, d with the baseline scenario (no coastal storm) (Fig. 11b) shows Q2 river flow on its own does not cause floods along the WFC. When Q2 simultaneously occurred with a regular W1, floods occur in the wetlands located around the western bank of the Muara Angke river inlet, which currently functions as a conservation area. Maximum water depth of 2.5 m occurred at the tip of Muara Angke. Most flooded areas were inundated up to around 0.5 m. Flood inundation increased with the severity of the coastal storm. From the more extreme W100, while flood depth and extent in the western side of the river inlet increased further, widespread inundation in the eastern side, where an extensive fishing population is located, can be seen. The

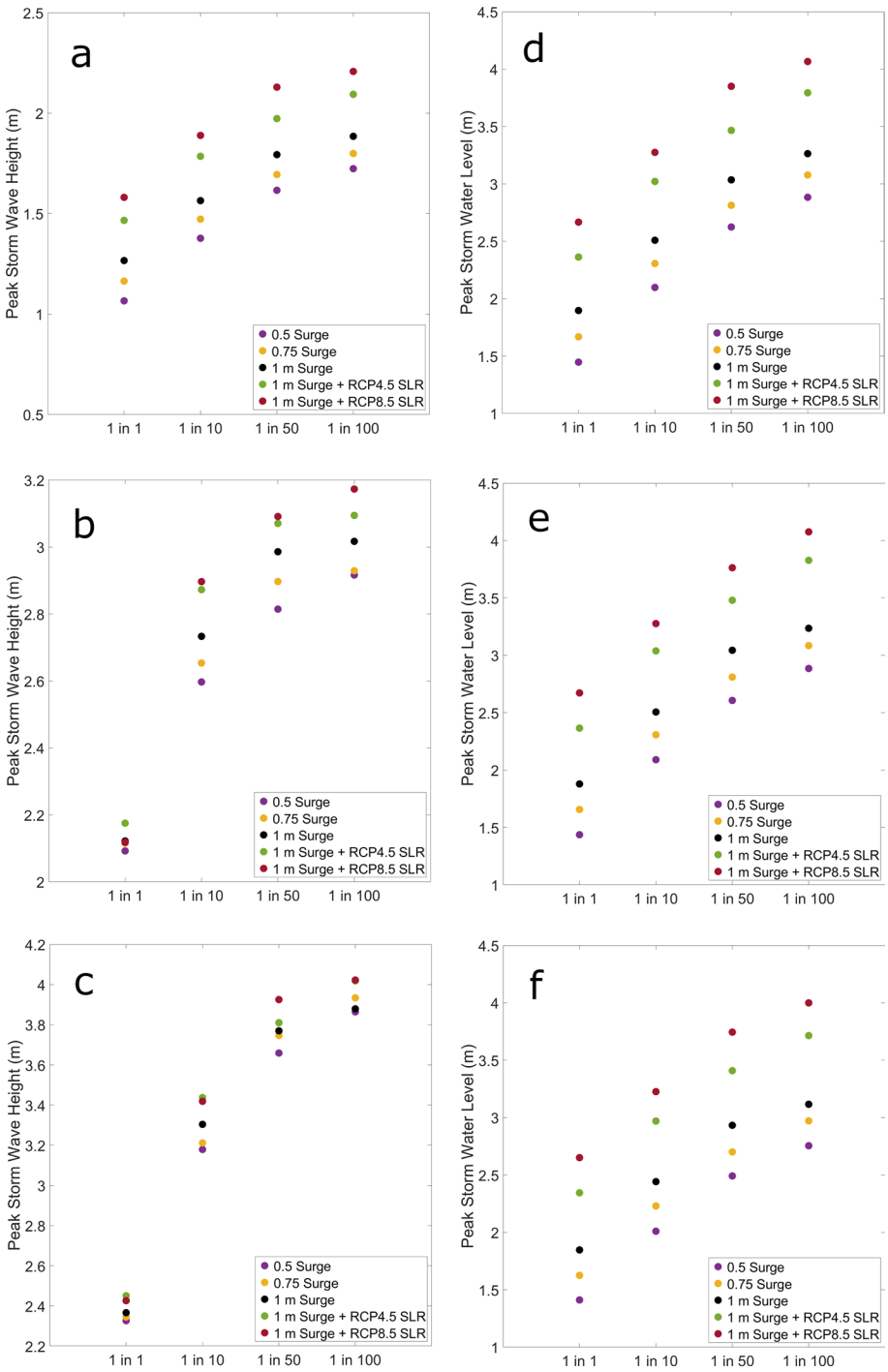


Fig. 10 Peak storm wave heights (a–c) and peak storm water levels (d–f) at P1, P2 and P3, respectively

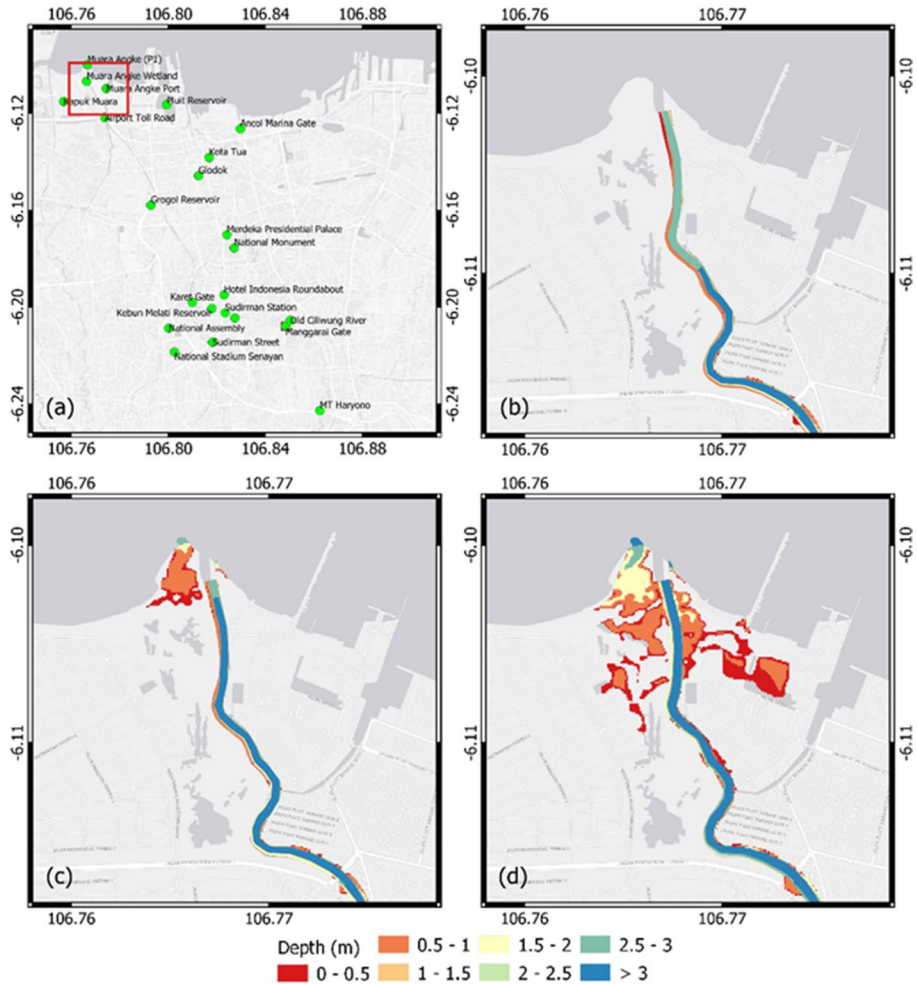


Fig. 11 a A map of Jakarta showing the modelled area in red; depth and extent of flooding around the West Flood Canal and Muara Angke river inlet from Q2 with **b** no coastal storm and 0 m surge (baseline scenario); **c** W1 and 0 m surge; **d** W100 and 0 m surge

maximum flood inundation depth reached 3 m while all wetland areas were inundated up to 1.5 m. The heavily populated surrounding areas both in the west and the east of the river inlet were inundated up to 1 m. A few localised places show up to 1.5 m inundation.

In addition to flood inundation found in the low-lying coastal areas, some localised inland flooding in Sudirman Station, Melati Reservoir, HI Roundabout in Central Jakarta, and the area adjacent to Karet Gate can be seen. However, these were not notably impacted by the severity of the coastal storm.

In Fig. 12c, d, flooding from W1 and W100 coastal storms when combined with the Q100 event is shown, alongside the baseline condition (Fig. 12b). Surge level was taken as 0 m. These results, when compared with floods from Q2 in Fig. 11b–d show that the spatial extent of flooding was not increased significantly by the increased river flow for the baseline and W1 conditions (Fig. 12b, c). However, for the W100 conditions there is

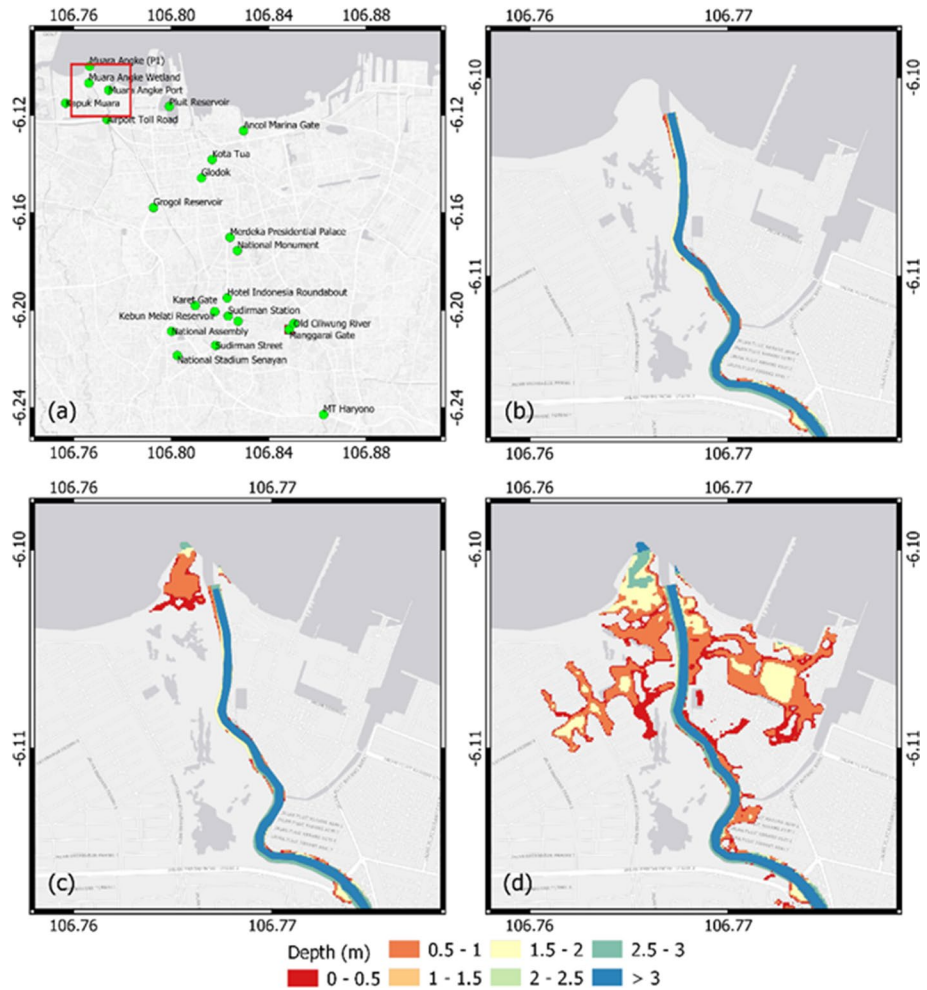


Fig. 12 Depth and extent of flooding around the West Flood Canal and Muara Angke river inlet from Q100 river discharge combined with coastal storms. **a** A map of Jakarta showing the modelled area in red; **b** no coastal storm and 0 m surge (baseline scenario); **c** W1 and 0 m surge; **d** W100 and 0 m surge

a large increase in flood extent (Fig. 12d). The overall flood inundation depths in most flooded areas have increased by 0.5–1 m on average from Q100. Flood inundation depth in the WFC and in a few localised areas inland surrounding Sudirman Station, Melati Reservoir, HI Roundabout in Central Jakarta, and the area adjacent to Karet Gate has increased with the increase in river flow. It should however be noted that this increase is small when compared to the increase in depth with the increase in severity of the coastal storm. These results highlight the fact that inland and coastal storms occur simultaneously even the most regular storm can lead to significant flooding in Muara Angke. The severity of flooding in this area is far more sensitive to coastal storm than the inland storm because of the elevated sea water level due to wind setup, even in the absence of a storm surge.

Storm surge can significantly increase the total water level during coastal low-pressure systems. Figure 13 shows flood inundation from the Q100 event combined with W1, and

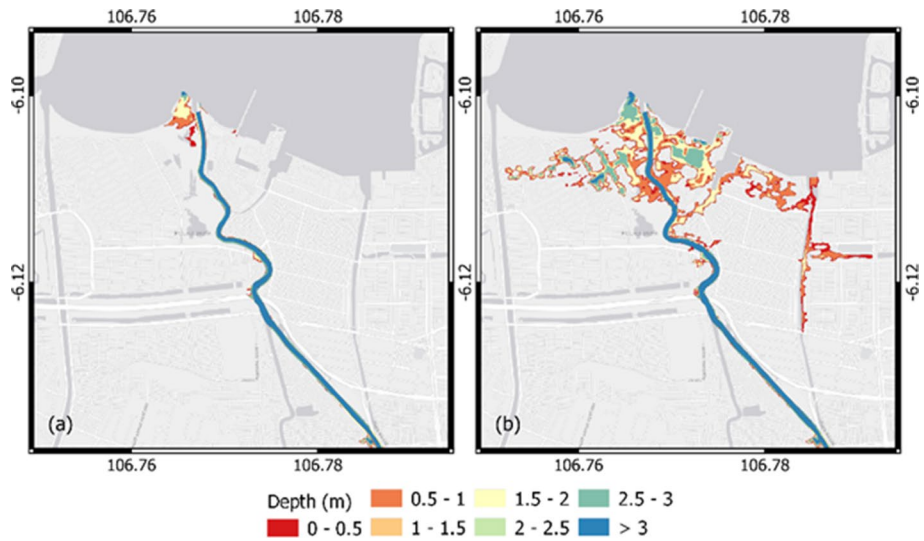


Fig. 13 Depth and extent of flooding around the West Flood Canal and Muara Angke river inlet from Q100 river discharge combined with coastal storms **a** W1, **b** W100, and 1 m surge

W100 coastal storms and 1 m surge. These scenarios resemble worst-case river flow and sea surge combined with regular, moderate, and severe coastal storms. Flooding from the Q100 combined with W1 and 1 m surge event generated substantially higher flood inundation depth at Muara Angke than that from the same events with 0 m surge (Fig. 12). On average, the water levels are 0.5–1 m higher. The extent of flooding is also higher where more land at the west of Muara Angke is inundated. No notable changes to flood inundation in the inland areas are seen. The flood scenarios Q100 combined with W100 and 1 m surge scenarios give rise to significantly higher floods. Flooding extends to greater areas westward and eastward of the river inlet as well as inland. Most inundated areas have water depths exceeding 1.5 m in W100 with a minimum flood depth exceeded 0.5 m.

Flooding varies across different flood scenarios. In addition to the intensity of the flood drivers, the ground topography also plays an important role when determining the extent of flooding and inundation depth. We investigate three key areas around the study site to assess flood characteristics. Figure 14 shows time variation of flood inundation depths at A1, a location in the vicinity of the Muara Angke Traditional Fish Market; A2, located in the wetlands of Muara Angke which directly floods from the sea; and A3, located at the urban settlement of Kapak Muara. A1 was flooded during high-intensity coastal storms. The inundation depth increases rapidly during the escalation of the storm and flood water stays in the area even after the subsidence of the storm due to poor drainage. The maximum inundation depth exceeded 3 m from the Q100/W100 event combined with 1 m surge. A2 was flooded from both regular and extreme events although floods recede quickly after the storm. The maximum inundation depth exceeded 3 m. A3 displays very similar characteristics to A1 except it was not flooded from events that combine regular inland and coastal storms. Floods are retained after the subsidence of a storm, which indicates poor drainage in this area.

In Fig. 15, the total inundated land area in Muara Angke surrounding the WFC due to combined floods is shown against peak flood water depth at the mouth of Muara Angke

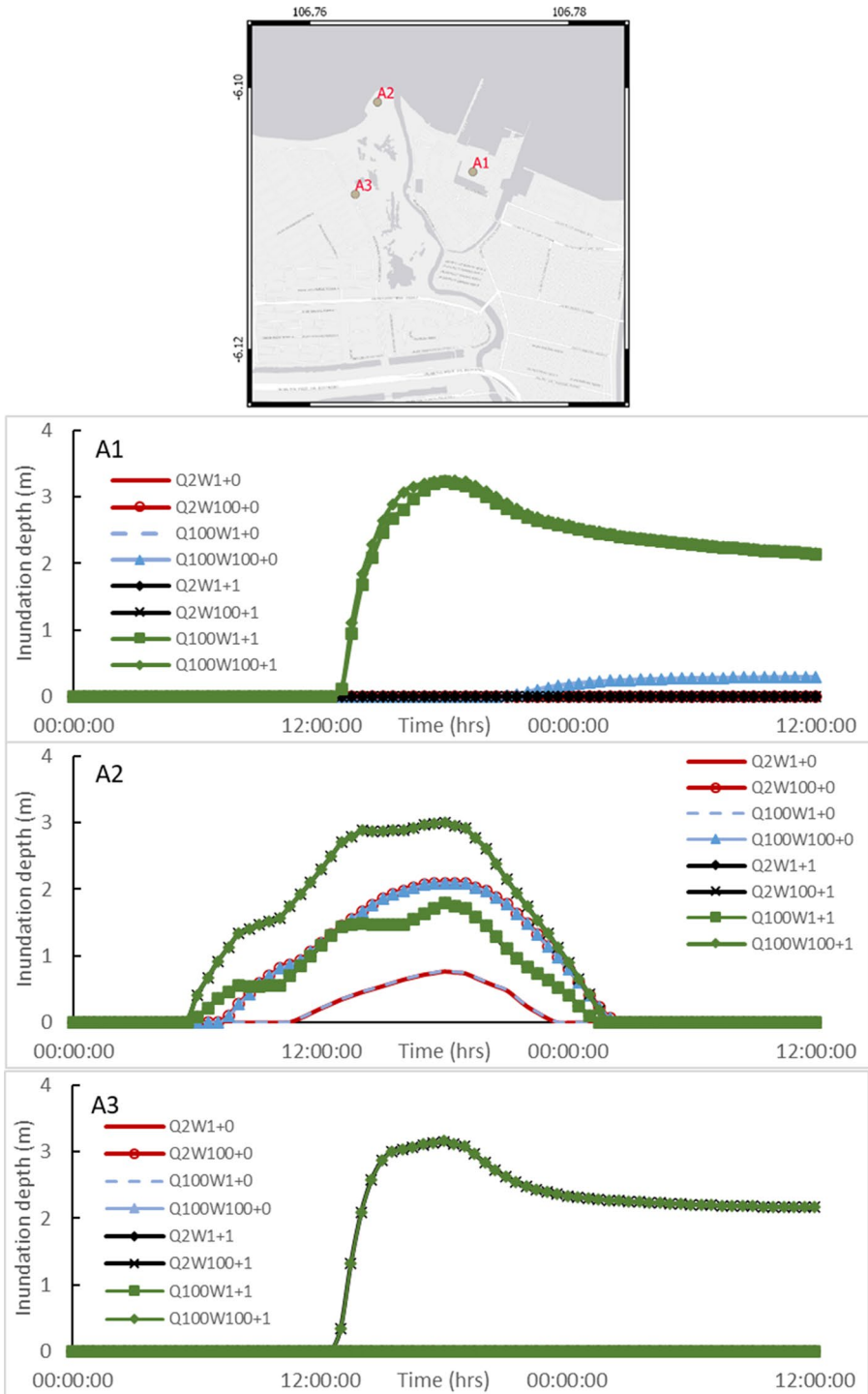
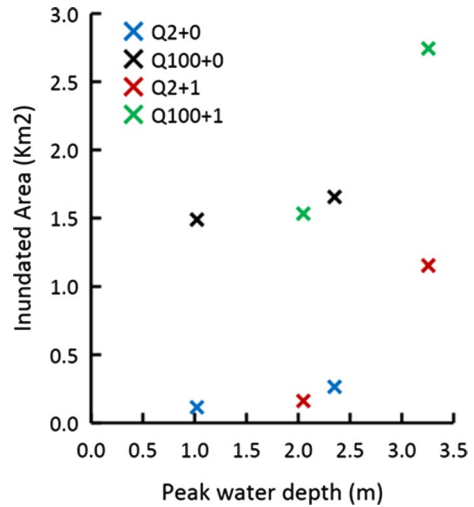


Fig. 14 Time-varying flood inundation depths at locations **A1** (vicinity of Muara Angke Traditional Fish Market); **A2** (at Muara Angke Wetland); and **A3** (at Kapuk Muara)

Fig. 15 Total inundated area surrounding WFC during W1, and W100 storms combined with Q2 and 0 m surge (blue), Q2 and 1 m surge (red), Q100 (black) and 0 m surge, and Q100 with 1 m surge (green)



river inlet. The extent of flooding is more sensitive to the severity of the coastal storm than the severity of the river discharge. When the sea water rises due to wind setup during a storm, water enters the areas not protected by sea defences. While flood depth gradually increases with the increase in severity of the coastal storm, the inundated area exponentially increases with the rise in coastal storm severity. A storm with 1 m surge can increase the inundated area in this part of Jakarta by three folds from that of without the surge, for the same peak fluvial discharge.

Coastal storms play a prominent role in flooding the low-lying areas surrounding Muara Angke river inlet although those areas do not flood directly due to overflowing from the sea. The crest level of most sea defences at Jakarta Bay currently stands at +4.8 m above mean sea level which is higher than the maximum water level observed during the rare W100 coastal storm combined with 1.0 m surge, which prevents flooding directly from the sea. The elevated sea water level due to wind and wave setup, combined with high river flow during simultaneously occurring coastal and inland storms are bound to inundate those areas around the river inlet as a result of overflowing of the banks of WFC. The severity of the coastal storm, and hence the increased sea water level, is found to be the primary factor that determines flood extent and inundation depth, although a small increase in flooding is observed with the increase of the severity of the inland storm. When the sea surge is superimposed with wind and wave setup, flooding exacerbates as a result of higher sea water level.

Jakarta has an extremely high rate of land subsidence. Although the rate varies with time and space, on average, subsidence of 5–15 cm/year has been reported in most parts of Jakarta (Abidin et al. 2010). Severe land subsidence, combined with rapidly rising sea level, forces Jakarta to be one of the fastest sinking cities around the world. To investigate the impacts of sea level rise and land subsidence on flooding around Muara Angke river inlet and wider areas of northern Jakarta, flood inundation at the end of this century (circa 2100) was simulated from a number of ‘future’ compound storm scenarios. In these simulations, relative sea level was derived by combining absolute sea level from RCP8.5 climate change scenario and a spatially uniform constant land subsidence rate of 10 cm/year.

Figure 16 shows inundation maps corresponding to flood events at the end of this century from Q2, combined with coastal storms W1, and W100 and, RCP4.5 and 8.5 SLR, 1.0 m surge, and land subsidence.

Figure 16 shows that land subsidence combined with SLR will submerge most of Jakarta by the end of this century, irrespective of both storm flooding and RCP scenario, at least if the spatially uniform current average land subsidence rate of 10 cm/year continues in the future and that coastal defences remain static. Flood inundation level varied with the severity of the coastal storm; however, the simulations show that most areas of Jakarta will be permanently under water. It may be noted that this may be an extreme scenario considering the fact that land subsidence is not spatially uniform, and that subsidence rate may be less than 10 cm/year in some areas of central and western Jakarta (Abidin et al. 2011).

The flooded areas surrounding WFC include the industrial warehousing area near Muara Angke, the Sunda Kelapa Port area and Kota Tua, and two heritage sites which are tourism

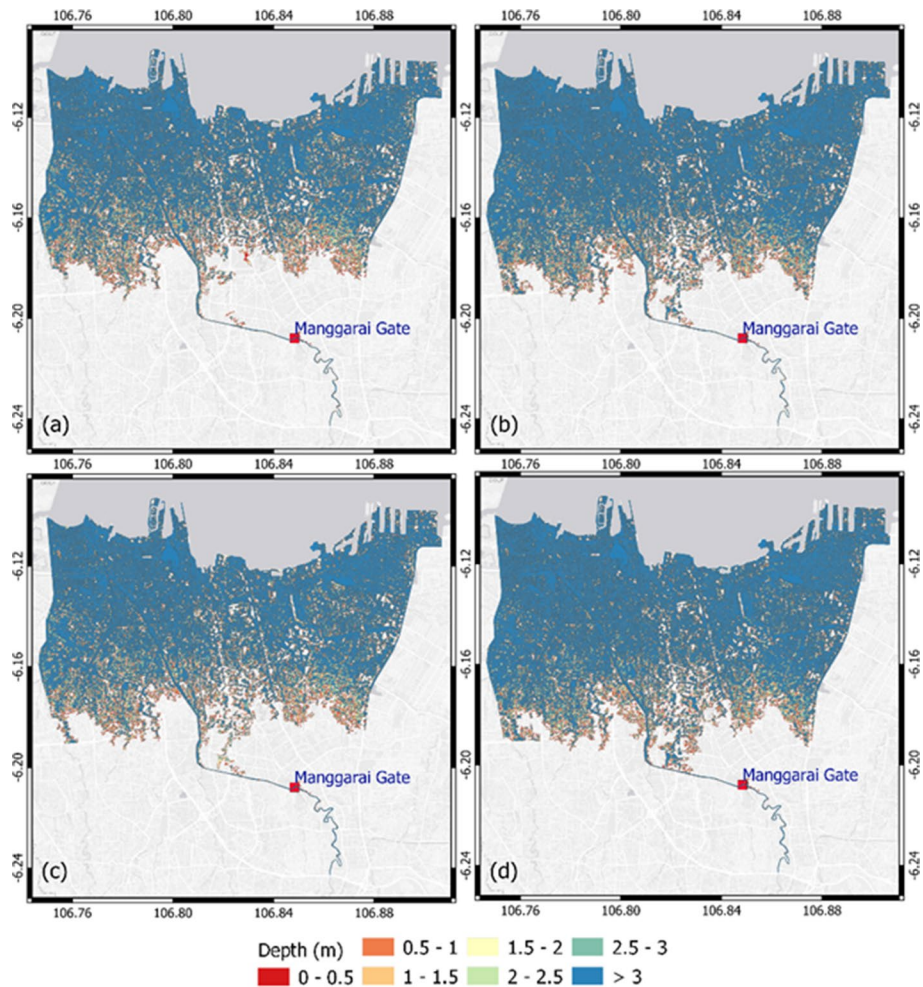


Fig. 16 Flood inundation maps corresponding to flood events from Q2 combined with coastal storms W1, W100 at the end of the century (circa 2100) under RCP4.5 (a, b) and RCP8.5 (c, d)

hotspots. The floods also inundate the Glodok and Ancol areas which are the economic and commercial hubs of northern Jakarta; access to the Sedyatmo toll road which functions as the airport toll road; and Pluit Reservoir which currently serves as a flood storage to control floods in the northern and central Jakarta, even reaching up to Merdeka Presidential Palace and the National Monument in Central Jakarta. Some areas will inundate up to 4 m while flood depth in many coastal areas far exceeds 4 m.

5 Conclusions

Compound flooding in Jakarta from a range of present and future storm conditions was modelled and analysed in this study. Flooding from both regular and rare storms were investigated. The hydrodynamic modelling results highlight the potential for substantial increases in peak water levels in Jakarta Bay during coastal storms due to wind and wave setup. Computational models did not simulate overflowing or wave induced overwashing of existing sea defences and hence direct coastal flooding under the current climate in areas protected by sea defences. The elevated water level in Jakarta Bay during storms as a result of wind and wave setup and sea surge acts as a barrier to the drainage of WFC that carry flood water from the Ciliwung river into Jakarta Bay. This phenomenon leads to water level in the WFC above its banks thus overflowing and inundating the areas surrounding the WFC and Muara Angke river inlet in northern Jakarta.

The most flood-prone areas are the highly populated fisherman's villages located in the low-lying areas to the west of Muara Angke river inlet, and wetlands adjacent to the river inlet that are not currently protected by flood defences. Under the compound events, flooding extended further inland into Sunda Kelapa port and beyond to the east and into the densely populated Kapok Muara to the west of the river inlet. Flood extent and inundation depths increase with the increase of the severity of flood drivers although the intensity of coastal storms play a greater role than the inland storm severity.

Future sea level rise due to climate change and on-going excessive land subsidence, combined with sea surge and elevated sea water levels due to wave and wind setup, generated mean sea water levels that surpass the crest height of current sea defences of Jakarta Bay shoreline. As a result, widespread flooding is predicted at the end of this century, mainly due to direct overflowing of coastal defences, regardless of the severity of inland and coastal storms. If the current rate of land subsidence and sea level rise continues in future, the majority of Jakarta will be permanently inundated by the end of this century.

It should be noted that flooding from only the simultaneous occurrence of coastal and inland storms, which is a common occurrence in this region, were investigated in this study. It was assumed that storm conditions will not significantly change in future. The study was primarily focused on the coastal areas impacted by the flood waters diverted from the Ciliwung river, which has the largest watershed in Jakarta. Pluvial input was not taken into account as it is much smaller compared to fluvial inputs. Numerous small drainage canals and flood control gates were not included in the models.

Our results show the important roles played by compound flood drivers when investigating flooding in the low-lying Muara Angke. The results also signify the importance of controlling seawater entering the river inlet during storms, and the need to strengthen coastal defences and improve the drainage to mitigate flooding and to minimise flood water retention time.

The simulation results provide an insights in to current and future compound flooding in the northern Jakarta which can assist assessments of flood risk and the development of sustainable flood risk management measures. The models and methods used in this study are directly transferable to investigate compound flooding from the sea and inland.

Finally, some limitations of this study should be noted. (1) we were unable to perform multivariate statistical analysis to investigate the dependence between different flood drivers and to generate statistically significant flood events due to lack of data. Therefore, univariate analysis on each flood driver was carried out and individual drivers with different return levels were combined to generate flood scenarios for numerical modelling; (2) sea surge data in Jakarta Bay was not available although eye-witness accounts of surges and approximated surge levels collected by the local research team. Synthetic surge profiles were generated using the limited available surge information; (3) the SLR data used for numerical modelling of future flooding was limited to RCP8.5 climate change scenario as our intention was to investigate future flooding from the worst-possible climate scenario; (4) Numerical simulations of flood inundation could not be validated quantitatively. Therefore, a qualitative comparison was made using a crude observed flood map during a flood event in 2020; and (5) the study was limited to Muara Angke and river input from the Ciliwung River diversion to West Flood Canal. Although a few other small rivers contribute to flooding of this site, no data were available to include them in the numerical model; (6) A comprehensive assessment of compound flooding for the whole of Jakarta is outside the scope of this study.

Acknowledgements This research was funded by the Natural Environment Research Council grant NE/S003282/1, the UK Newton Fund, the UK Economic and Social Research Council, and the Ministry of Research, Technology & Higher Education of the Republic of Indonesia (RISTEK-BRIN). This research utilises data from BMKG (Badan Meteorologi Klimatologi dan Geofisika), BBWS CiliCis (Balai Besar Wilayah Sungai Ciliwung Cisadane), BAPPENAS (Badan Perencanaan Pembangunan Nasional). We acknowledge the support of the Supercomputing Wales project, which is part-funded by the European Regional Development Fund (ERDF) via the Welsh Government.

Authors contributions Conceptualization: [HK, HPR, RH, MSBK, DA]; methodology: [HK, WGB, YX, MSBK, MF]; formal analysis and investigation: [WGB, AAK, BK, DS, TN, AK]; writing—original draft preparation: [HK, WGB]; writing—review and editing: [HK, YX, RH]; funding acquisition: [RH, HK, HPR, DA]; supervision: [HK, RH, MSBK, MF].

Funding This research was funded by the Natural Environment Research Council Grant NE/S003282/1, the UK Newton Fund, the UK Economic and Social Research Council, and the Ministry of Research, Technology & Higher Education of the Republic of Indonesia (RISTEK-BRIN).

Data availability statement The data that support this study, including all model inputs and outputs are available from the Zenodo repository: <https://doi.org/10.5281/zenodo.7848187>.

Declarations

Conflict of interest The authors have no relevant financial or non-financial interests to disclose.

Open Access This article is licensed under a Creative Commons Attribution 4.0 International License, which permits use, sharing, adaptation, distribution and reproduction in any medium or format, as long as you give appropriate credit to the original author(s) and the source, provide a link to the Creative Commons licence, and indicate if changes were made. The images or other third party material in this article are included in the article's Creative Commons licence, unless indicated otherwise in a credit line to the material. If material is not included in the article's Creative Commons licence and your intended use is not permitted by statutory regulation or exceeds the permitted use, you will need to obtain permission directly from the copyright holder. To view a copy of this licence, visit <http://creativecommons.org/licenses/by/4.0/>.

References

- Abidin HZ, Djaja R, Darmawan D, Hadi S, Akbar A, Rajiyowiryono H, Sudibyo Y, Meilano I, Kusuma MA, Kahar J, Subarya C (2001) Land subsidence of Jakarta (Indonesia) and its geodetic monitoring system. *Nat Hazards* 23:365–387. <https://doi.org/10.1023/A:1011144602064>
- Abidin HZ, Andreas H, Gamal M, Gumilar I, Napitupulu N, Fukuda Y, Deguchi T, Maruyama Y, Riawan E (2010) Land subsidence characteristics of the Jakarta basin (Indonesia) and its relation with groundwater extraction and sea level rise. In: Taniguchi M, Holman IP (eds) *Groundwater response to changing climate*. CRC Press, Boca Raton, pp 113–130. <https://doi.org/10.1201/b10530-11>
- Abidin HZ, Andreas H, Gumilar I, Fukuda Y, Pohan YE, Deguchi T (2011) Land subsidence of Jakarta (Indonesia) and its relation with urban development. *Nat Hazards* 59:1753–1771
- Adytia D, Saepudin D, Pudjuprasedya SR, Husrin S, Sopaheluwakan A (2022) A deep learning approach for wave forecasting based on a spatially correlated wind feature, with a case study in the Java Sea, Indonesia. *Fluids* 7:39
- Akmalah E, Grigg NS (2011) Jakarta flooding: systems study of socio- technical forces. *Water Int* 36(6):733–747. <https://doi.org/10.1080/02508060.2011.610729>
- Alsaaq F, Shamji VR (2022) Extreme wind wave climate off Jeddah Coast, the Red Sea. *J Mar Sci Eng.* <https://doi.org/10.3390/jmse10060748>
- Badan Informasi Geospasial (2018) DEMNAS seamless digital elevation model (DEM) dan Batimetri Nasional. <https://tanahair.indonesia.go.id/demnas/>
- Bermúdez M, Farfán JF, Willems P, Cea L (2021) Assessing the effects of climate change on compound flooding in coastal river areas. *Water Resour Res* 57:1–19. <https://doi.org/10.1029/2020WR029321>
- Bevacqua E, Maraun D, Hobæk Haff I, Widmann M, Vrac M (2017) Multivariate statistical modelling of compound events via pair-copula constructions: analysis of floods in Ravenna (Italy). *Hydrol Earth Syst Sci* 21(6):2701–2723
- Bhaskaran PK, Gupta N, Dash MK (2014) Wind-wave climate projections for the Indian Ocean from satellite observations. *J Mar Sci Res Dev* S11:005. <https://doi.org/10.4172/2155-9910.S11-005>
- Budiyono Y, Aerts J, Brinkman JJ, Marfai MA, Ward P (2015) Flood risk assessment for delta mega-cities: a case study of Jakarta. *Nat Hazards* 75(1):389–413. <https://doi.org/10.1007/s11069-014-1327-9>
- Budiyono Y, Aerts J, Tollenaar D, Ward PJ (2016) River flood risk in Jakarta under scenarios of future change. *Nat Hazard* 16:757–774
- Camus P, Haigh ID, Nasr AA, Wahl T, Darby SE, Nicholls RJ (2021) Regional analysis of multivariate compound coastal flooding potential around Europe and environs: sensitivity analysis and spatial patterns. *Nat Hazard* 21:2021–2040. <https://doi.org/10.5194/nhess-21-2021-2021>
- Coles S (2001) *An introduction to statistical modeling of extreme values*. Springer, London
- Couason A, Eilander D, Muis S, Veldkamp TI, Haigh ID, Wahl T, Winsemius HC, Ward PJ (2020) Measuring compound flood potential from river discharge and storm surge extremes at the global scale. *Nat Hazard* 20(2):489–504
- Defant A (1961) *Physical oceanography*. Pergamon Press, New York
- Del-Rosal-Salido J, Folgueras P, BermúdezOrtega-Sánchez MM, Losada MA (2021) Flood management challenges in transitional environments: assessing the effects of sea-level rise on compound flooding in the 21st century. *Coast Eng* 167:103872
- Deltares (2009) *Flood hazard mapping 2—overview*. Report number Q0743.00. Deltares, Delft
- Deltares (2022) *Delft3D_Flow, simulation of multi-dimensional hydrodynamic flows and transport phenomena, including sediments, user Manual*
- Egbert GD, Erofeeva SY (2002) Efficient inverse modeling of barotropic ocean tides. *J Atmos Ocean Technol* 19(2):183–204. [https://doi.org/10.1175/1520-0426\(2002\)019%3c0183:EIMOBO%3e2.0.CO;2](https://doi.org/10.1175/1520-0426(2002)019%3c0183:EIMOBO%3e2.0.CO;2)
- Eilander D, Couason A, Ikeuchi H, Muis S, Yamazaki D, Winsemius HC, Ward PJ (2020) The effect of surge on riverine flood hazard and impact in deltas globally. *Environ Res Lett* 15(10):104007
- Emam AR, Mishra BK, Kumar P, Masago Y, Fukushi K (2016) Impact assessment of climate and land-use changes on flooding behavior in the upper Ciliwung River, Jakarta, Indonesia. *Water* 8(12):559
- Farid M, Saputra D, Maitsa TR, Kesuma TNA, Kuntoro AA, Chrysanti A (2021) Relationship between extreme rainfall and design flood-discharge of the Ciliwung River. *IOP Conf Ser Earth Environ Sci* 708:012031
- Formánek A, Silasari R, Kusuma MSB, Kardhana H (2014) Two-dimensional model of Ciliwung river flood in DKI Jakarta for development of the regional flood index map. *J Eng Technol Sci* 45(3):307–325
- GEBCO Compilation Group (2019) GEBCO 2019 Grid. <https://doi.org/10.5285/836f016a-33be-6ddc-e053-6c86abc0788e>
- Ghanbari M, Arabi M, Kao S-C, Obeysekera J, Sweet W (2021) Climate change and changes in compound coastal-riverine flooding hazard along the U.S. coasts. *Earth's Future* 9:e2021EF002055

- Gori A, Lin N (2022) Projecting compound flood hazard under climate change with physical models and joint probability methods. *Earth's Future*. <https://doi.org/10.1029/2022EF003097>
- Gori A, Lin N, Smith J (2020a) Assessing compound flooding from landfalling tropical cyclones on the North Carolina Coast. *Water Resour Res*. <https://doi.org/10.1029/2019WR026788>
- Gori A, Lin N, Xi D (2020b) Tropical cyclone compound flood hazard assessment: from investigating drivers to quantifying extreme water levels. *Earth's Future*. <https://doi.org/10.1029/2020EF001660>
- Gori A, Lin N, Xi D, Emanuel K (2022) Tropical cyclone climatology change greatly exacerbates US extreme rainfall-surge hazard. *Nat Clim Change* 12:171–178
- Guo Y, Hou Y, Liu Z, Du M (2020) Risk prediction of coastal hazards induced by Typhoon: a case study in the coastal region of Shenzhen, China. *Remote Sens*. <https://doi.org/10.3390/rs12111731>
- Hallegette S, Green C, Nicholls RJ, Corfee-Morlot J (2013) Future flood losses in major coastal cities. *Nat Clim Change* 3:802–806. <https://doi.org/10.1038/nclimate1979>
- Hanson S, Nicholls R, Ranger N, Hallegette S, Corfee-Morlot J, Herweijer C, Chateau J (2011) A global ranking of port cities with high exposure to climate extremes. *Clim Change* 104:89–111. <https://doi.org/10.1007/s10584-010-9977-4>
- Hawkes PPJ, Gouldby BPB, Tawn JA, Owen MW (2002) The joint probability of waves and water levels in coastal engineering design. *J Hydraul Res* 40:241–251. <https://doi.org/10.1080/00221680209499940>
- Hendry A, Haigh ID, Nicholls RJ, Winter H, Neal R, Wahl T, Joly-Lauge A, Darby SE (2019) Assessing the characteristics and drivers of compound flooding events around the UK coast. *Hydrol Earth Syst Sci* 23:3117–3139. <https://doi.org/10.5194/hess-23-3117-2019>
- Hersbach H, Bell B, Berrisford P, Biavati G, Horányi A, Muñoz Sabater J, Nicolas J, Peubey C, Radu R, Rozum I, Schepers D, Simmons A, Soci C, Dee D, Thépaut J-N (2018) ERA5 hourly data on single levels from 1979 to present. Copernicus Climate Change Service (C3S) Climate Data Store (CDS). Accessed on 30 Oct 2019. <https://doi.org/10.24381/cds.adbb2d47>.
- Hunt JC (2005) Inland and coastal flooding: developments in prediction and prevention. *Philos Trans R Soc A Math Phys Eng Sci* 363(1831):1475–1491
- IPCC (2012) Managing the risks of extreme events and disasters to advance climate change adaptation. A special report of working groups I and II of the Intergovernmental Panel on Climate Change. Cambridge University Press, Cambridge.
- Jagger TH, Elsner JB (2006) Climatology models for extreme hurricane winds near the United States. *J Clim* 19:3220–3236
- Jamalludin J, Fatoni KI, Alam TM, Pranowo WS (2016) Identifikasi Banjir Rob Periode 2013–2015 Di Kawasan Pantai Jakarta Utara Jakarta. *Jurnal Chart Datum* 2:105–116
- Jane R, Cadavid L, Obeysekera J, Wahl T (2020) Multivariate statistical modelling of the drivers of compound flood events in south Florida. *Nat Hazards Earth Syst Sci* 20:2681–2699. <https://doi.org/10.5194/nhess-20-2681-2020>
- Kim H, Villarini G, Jane R, Wahl T, Misra S, Michalek A (2023) On the generation of high-resolution probabilistic design events capturing the joint occurrence of rainfall and storm surge in coastal basins. *Int J Clim* 43(2):761–771. <https://doi.org/10.1002/joc.7825>
- Kumbier K, Carvalho RC, Vafeidis AT, Woodroffe CD (2018) Investigating compound flooding in an estuary using hydrodynamic modelling: a case study from the Shoalhaven River, Australia. *Nat Hazards Earth Syst Sci* 18(2):463–477. <https://doi.org/10.5194/nhess-18-463-2018>
- Kupfer S, Santamaria-Aguilar S, Van Niekerk L, Lück-Vogel M, Vafeidis AT (2022) Investigating the interaction of waves and river discharge during compound flooding at Breede River inlet, South Africa. *Nat Hazards Earth Syst Sci* 22:187–205. <https://doi.org/10.5194/nhess-22-187-2022>
- Kusuma MSB, Rahayu HP, Farid M, Adityawan MB, Setiawati T, Silasari R (2010) Studi Pengembangan Peta Indeks Resiko Banjir pada Kelurahan Bukit Duri Jakarta. *Jurnal Teknik Sipil* 17(2):123–134
- Lai Y, Li Q, Li J, Zhou Q, Zhang X, Wu G (2021) Evolution of frequency and intensity of concurrent heavy precipitation and storm surge at the global scale: Implications for compound floods. *Earth Sci Front*. <https://doi.org/10.3389/feart.2021.660359>
- Larasari AA, Husrin S, Bachtiar H, Sembiring LE (2018) Preliminary studies of dyke prodiles for Jakarta outer sea dike: physical model test results. In: Proceedings of 21st IAHR-APD Congress, Yogyakarta, Indonesia
- Lesser GR, Roelvink JA, van Kester JATM, Stelling GS (2004) Development and validation of a three-dimensional morphological model. *Coast Eng* 51:883–915
- Lian JJ, Xu K, Ma C (2013) Joint impact of rainfall and tidal level on flood risk in a coastal city with a complex river network: a case study of Fuzhou City, China. *Hydrol Earth Syst Sci* 17:679–689
- Liu Q, Xu H, Wang J (2022) Assessing tropical cyclone compound flood risk using hydrodynamic modelling: a case study in Haikou City, China. *Nat Hazards Earth Syst Sci* 22(2):665–675. <https://doi.org/10.5194/nhess-22-665-2022>

- Lubis SW, Hagos S, Hermawan E, Respati MR, Ridho A, Risyanto, et al (2022) Record-breaking precipitation in Indonesia's capital of Jakarta in early January 2020 linked to the northerly surge, equatorial waves, and MJO. *Geophys Res Lett* 49:e2022GL101513. <https://doi.org/10.1029/2022GL101513>
- Lucey JTD, Gallien TW (2022) Characterizing multivariate coastal flooding events in a semi-arid region: the implications of copula choice, sampling, and infrastructure. *Nat Hazards Earth Syst Sci* 22:2145–2167. <https://doi.org/10.5194/nhess-22-2145-2022>
- Machado AA, Calliari LJ (2016) Synoptic systems generators of extreme wind in Southern Brazil: atmospheric conditions and consequences in the coastal zone. *J Coast Res* 1(75):1182–1186. <https://doi.org/10.2112/SI75-237.1>
- McMillan A, Batstone C, Worth D, Tawn J, Horsburgh K, Lawless M (2011) Coastal flood boundary conditions for UK Mainland and Islands. https://www.gov.uk/government/uploads/system/uploads/attachment_data/file/291216/scho0111btki-e-e.pdf
- Mishra BK, Rafiei Emam A, Masago Y, Kumar P, Regmi RK, Fukushi K (2018) Assessment of future flood inundations under climate and land use change scenarios in the Ciliwung River Basin, Jakarta. *J Flood Risk Manag* 11:S1105–S1115
- Moftakhari HR, AghaKouchak A, Sanders BF, Allaire M, Matthew RA (2018) What is nuisance flooding? Defining and monitoring an emerging challenge. *Water Resour Res* 54(7):4218–4227. <https://doi.org/10.1029/2018WR022828>
- Moss R, Babiker M, Brinkman S, Calvo E, Carter TR, Edmonds J, Elgizouli I, Emori S, Erda L, Hibbard K, Jones R, Kainuma M, Kelleher J, Lamarque J-F, Manning MR, Matthews B, Meehl J, Meyer L, Mitchell JFB, Nakicenovic N, O'Neill B, Pichs R, Riahi K, Rose SK, Runci P, Stouffer RJ, van Vuuren DP, Weyant JP, Wilbanks TJ, van Ypersele JP, Zurek M (2008). Towards new scenarios for analysis of emissions, climate change, impacts, and response strategies: IPCC Expert Meeting Report, 19–21 September 2007. Noordwijkerhout, The Netherlands, p 155
- Moss RH, Edmonds JA, Hibbard KA, Manning MR, Rose SK, van Vuuren DP, Carter TR, Emori S, Kainuma M, Kram T, Meehl GA, Mitchell JFB, Nakicenovic N, Riahi K, Smith SJ, Stouffer RJ, Thomson AM, Weyant JP, Wilbanks TJ (2010) The next generation of scenarios for climate change research and assessment. *Nature* 463(7282):747–756
- Muñoz DF, Yin D, Bakhtyar R, Moftakhari H, Xue Z, Mandli K, Ferreira C (2022) Inter-model comparison of Delft3D-FM and 2D HEC-RAS for total water level prediction in coastal to inland transition zones. *J Am Water Res Assoc* 58(1):34–49. <https://doi.org/10.1111/1752-1688.12952>
- Niroomandi A, Ma G, Ye X, Lou S, Xue P (2018) Extreme value analysis of wave climate in Chesapeake Bay. *Ocean Eng* 159:22–36. <https://doi.org/10.1016/j.oceaneng.2018.03.094>
- Olbert A, Comer J, Nash S, Hartnett M (2017) High-resolution multi-scale modelling of coastal flooding due to tides, storm surges and rivers inflows. *A Cork City. Ex Coast Eng* 121:278–296. <https://doi.org/10.1016/j.coastaleng.2016.12.006>
- Oppenheimer M, Glavovic B (2019) Chapter 4: Sea level rise and implications for low lying islands, coasts and communities. In: Pörtner H-O, Roberts DC, Masson-Delmotte V, Zhai P, Tignor M, Poloczanska E, Mintenbeck K, Nicolai M, Okem A, Petzold J, Rama B, Weyer N (eds) IPCC SR ocean and cryosphere. IPCC special report on the ocean and cryosphere in a changing climate. Cambridge University Press, Cambridge, pp 1–14
- Pasquier U, He Y, Hooton S, Goulden M, Hiscock KM (2019) An integrated 1D–2D hydraulic modelling approach to assess the sensitivity of a coastal region to compound flooding hazard under climate change. *Nat Hazards* 98:915–937
- Pender D, Karunarathna H (2013) A statistical-process based approach for modelling beach profile variability. *Coast Eng* 81:19–29. <https://doi.org/10.1016/j.coastaleng.2013.06.006>
- Petroliagkis TI, Voukouvalas E, Disperati J, Bidlot J (2016) Joint probabilities of storm surge, significant wave height and river discharge components of coastal flooding events. Joint Research Centre
- Priyambodoho BA, Kure S, Yagi R, Januriyadi NF (2021) Flood inundation simulations based on GSMaP satellite rainfall data in Jakarta, Indonesia. *Prog Earth Planet Sci* 8:34
- Rusdiansyah A, Tang Y, He Z, Li L, Ye Y, Yahya Surya M (2018) The impacts of the large-scale hydraulic structures on tidal dynamics in open-type bay: numerical study in Jakarta Bay. *Ocean Dyn* 68(9):1141–1154
- Rustiadi E, Pravitasari AE, Setiawan Y, Mulya SP, Pribadi DO, Tsutsumida N (2021) Impact of continuous Jakarta megacity urban expansion on the formation of the Jakarta–Bandung conurbation over the rice farm regions. *Cities* 111:103000. <https://doi.org/10.1016/j.cities.2020.103000>
- Sagala S, Lassa J, Yasaditama H, Hudalah D (2013) The evolution of risk and vulnerability in Greater Jakarta: contesting government policy in dealing with a megacity's exposure to flooding, An

- academic response to Jakarta Floods in January 2013, IRGSC working paper no. 2, Institute of Resource Governance and Social Change (IRGSC), Kupang, pp 1–18
- Shen Y, Morsy MM, Huxley C, Tahvildari N, Goodall JL (2019) Flood risk assessment and increased resilience for coastal urban watersheds under the combined impact of storm tide and heavy rainfall. *J Hydrol* 579:124159. <https://doi.org/10.1016/j.jhydrol.2019.124159>
- Surya MY, He Z, Xia Y, Li L (2019) Impacts of sea level rise and river discharge on the hydrodynamics characteristics of Jakarta Bay (Indonesia). *Water* 11(7):1384
- Tessler ZD, Vorosmarty CJ, Grossberg M, Gladkova I, Aizenman H, Syvitski JPM, Foufoula-Georgiou E (2015) Profiling risk and sustainability in coastal deltas of the world. *Science* 80(349):638–643. <https://doi.org/10.1126/science.aab3574>
- Texier P (2008) Floods in Jakarta: when the extreme reveals daily structural constraints and mismanagement. *Disaster Prev Manag* 17(3):358–372
- Van Voorst R, Hellman J (2015) One risk replaces another. *Asian J Soc Sci* 43:786–810. <https://doi.org/10.1163/15685314-04306007>
- Wahl T, Jain S, Bender J, Meyers SD, Luther ME (2015) Increasing risk of compound flooding from storm surge and rainfall for major US cities. *Nat Clim Chang* 5(12):1093–1097. <https://doi.org/10.1038/nclimate2736>
- Ward PJ, Marfai MA, Yulianto F, Hizbaro DR, Aerts JCJH (2011a) Coastal inundation and damage exposure estimation: a case study for Jakarta. *Nat Hazards* 56:899–916. <https://doi.org/10.1007/s11069-010-9599-1>
- Ward PJ, De Moel H, Aerts JCJH (2011b) How are flood risk estimates affected by the choice of return-periods? *Nat Hazards Earth Syst Sci* 11:3181–3195. <https://doi.org/10.5194/nhess-11-3181-2011>
- Ward PJ, Budiyo Y, Marfai MA (2013) Flood risk in Jakarta. In: Kron W, Apel H (eds) Severe weather in Eastern Asia. Perils, risks, insurance. Munich Re Knowledge Series Natural Hazards. Munich Re, Munich, pp 106–107
- Ward PJ, Couasnon A, Eilander D, Haigh ID, Hendry A, Muis S, Veldkamp TI, Winsemius HC, Wahl T (2018) Dependence between high sea-level and high river discharge increases flood hazard in global deltas and estuaries. *Environ Res Lett* 13(8):084012
- Wicaksono A, Herdiansyah H (2019) The impact analysis of flood disaster in DKI Jakarta: prevention and control perspective. *J Phys Conf Ser* 1339(1):012092. <https://doi.org/10.1088/1742-6596/1339/1/012092>
- Wijayanti P, Zhu X, Hellegers P, Budiyo Y, van Ierland EC (2017) Estimation of river flood damages in Jakarta, Indonesia. *Nat Hazards* 86:1059–1079

Publisher's Note Springer Nature remains neutral with regard to jurisdictional claims in published maps and institutional affiliations.